

π parameters in $\text{LM}(\text{CO})_5$ systems, but of the compounds discussed here, only $\text{Mo}(\text{CO})_5\text{P-}n\text{-Bu}_3$ was studied. Bodner and co-workers³⁰ have inferred relative donor:acceptor abilities for a number of ligands by examining the carbonyl ^{13}C chemical shifts of a large number of $\text{LM}(\text{CO})_n$ complexes. Their results are in accord with those presented here; i.e., the donor-acceptor ratios of alkylphosphines increases in the order $\text{PMe}_3 < \text{PEt}_3 < \text{P-}n\text{-Bu}_3$.

The parameter a listed in Table III for each series should correspond to the first ionization potential of the homoleptic hexakis(phosphine) complex $\text{Mo}(\text{PR}_3)_6$. Although it is likely that these would not be stable for alkylphosphines, it is of interest to note that $\text{P-}n\text{-Bu}_3$ is a stronger enough donor than PMe_3 that the ionization potential of $\text{Mo}(\text{P-}n\text{-Bu}_3)_6$ is predicted to be nearly 1 eV lower than that of $\text{Mo}(\text{PMe}_3)_6$.

Future Considerations. The application of the ligand additivity model to PES data allows, in principle, the direct determination of ligand bonding capabilities by using the energetic effects of ligands upon d orbitals. As the observed magnitudes of change in the ionization potentials indicate, this is more sensitive than investigating a ligand's influence indirectly by, for example, observing the change in CO stretching frequency induced by the ligand. In addition, it is not necessary to have homologous systems for different ligands; the ligand additivity parameters a , b , and c can be uniquely de-

termined from several different combinations of substituted systems. As an example, a comparison of the PE spectra of ML_6 and $\text{ML}_5\text{L}'$ would directly yield b and $b + c$, from which all these parameters can be derived.

The model will achieve even greater utility when the relationship between b and c is determined. Since b represents a combined σ and π influence whereas c is π only, it should be possible to achieve true separation of σ and π effects through the proper comparison of b and c . Our efforts to achieve this are ongoing.

Acknowledgment. The authors wish to acknowledge the Department of Energy (Contract DE-AC02-80ER10746), the Robert A. Welch Foundation, the University of Arizona, and The Ohio State University for partial support of this research.

Note Added in Proof. A recent communication by Bancroft et al.³¹ reports the PE spectra of $\text{W}(\text{CO})_6$, $\text{W}(\text{CO})_5\text{PMe}_3$, $\text{W}(\text{CO})_5\text{PEt}_3$, *cis*- $\text{W}(\text{CO})_4(\text{PMe}_3)_2$, *trans*- $\text{W}(\text{CO})_4(\text{PMe}_3)_2$, *trans*- $\text{W}(\text{CO})_4(\text{PEt}_3)_2$, and *fac*- $\text{W}(\text{CO})_3(\text{PMe}_3)_3$ and the correlation of these within the ligand additivity model. Their results provide further strong experimental support for the validity of the model.

Registry No. $\text{Mo}(\text{CO})_6$, 13939-06-5; $\text{Mo}(\text{CO})_5(\text{PMe}_3)$, 16917-96-7; *cis*- $\text{Mo}(\text{CO})_4(\text{PMe}_3)_2$, 16027-45-5; *trans*- $\text{Mo}(\text{CO})_4(\text{PMe}_3)_2$, 30513-03-2; *fac*- $\text{Mo}(\text{CO})_3(\text{PMe}_3)_3$, 19195-94-9; $\text{Mo}(\text{CO})_5(\text{PEt}_3)$, 19217-79-9; *trans*- $\text{Mo}(\text{CO})_4(\text{PEt}_3)_2$, 19217-81-3; $\text{Mo}(\text{CO})_5(\text{PBu}_3)$, 15680-62-3; *trans*- $\text{Mo}(\text{CO})_4(\text{PBu}_3)_2$, 17652-79-8.

(30) Bodner, G. M.; May, M. P.; McKinney, L. E. *Inorg. Chem.* 1980, 19, 1951-1958.

(31) Bancroft, G. M.; Dignard-Bailey, L.; Puddephatt, R. J. *Inorg. Chem.* 1984, 23, 2369-2370.

Contribution from the Institute of Inorganic Chemistry, University of Frankfurt, D-6000 Frankfurt, West Germany

Gas-Phase Reactions. 44.¹ The $\text{P}_4 \rightleftharpoons 2\text{P}_2$ Equilibrium Visualized^{2,3}

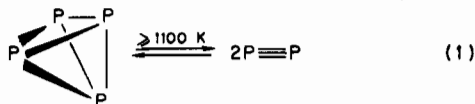
H. BOCK* and H. MÜLLER⁴

Received January 20, 1984

Photoelectron spectroscopic molecular fingerprints and their intensity variations during reactions have been used to determine the temperature dependence of the $\text{P}_4 \rightleftharpoons 2\text{P}_2$ equilibrium constant, $\ln K_p = -27870(1/T) + 12.90$, with a correlation coefficient $R = 0.995$. A MNDO total energy hypersurface helps to further visualize the $T_d \rightarrow D_{2d}$ symmetry-forbidden dissociation into 2P_2 and their reverse combination to white phosphorus.

Introduction

In the gas phase, the P_4 tetrahedron decomposes at temperatures above 1100 K into two P_2 fragments⁵ (eq 1). The



dissociation energy, $D_0 = 217 \text{ kJ/mol}$,⁶ is used to produce the then stable diatomic species P_2 , iso(valence)-electronic to the

nitrogen molecule, by formally breaking four PP bonds while two are shortened from 221 pm⁵ to 189 pm.⁶

Both element modifications (eq 1) have been investigated repeatedly by photoelectron (PE) spectroscopy,⁷⁻¹² and the observed ionization patterns are assigned to the radical-cat-

(1) Part 43: Bock, H.; Haun, M.; Mintzer, J. *Abstr. 8th Int. Congr. Catal.* 1984, 5, 691.

(2) For a review of PES-optimized gas-phase reactions containing a preliminary communication, cf.: Bock, H.; Solouki, B. *Angew. Chem.* 1981, 93, 425; *Angew. Chem., Int. Ed. Engl.* 1981, 20, 427.

(3) For gas-phase reactions of P_4 and P_2 cf.: Bock, H.; Wittmann, J.; Müller, H. *Chem. Ber.* 1982, 115, 2338.

(4) Müller, H. Ph. D. Thesis, University of Frankfurt, 1980.

(5) Cf. e.g.: "Gmelins Handbuch der Anorganischen Chemie"; Verlag Chemie: Weinheim, 1964; Phosphorus, Vol. B-8.

(6) McBride, B. J.; Heimel, S.; Ehlers, J. G.; Cordon, S. *NASA [Spec. Publ.] SP NASA SP-3001*, 257.

(7) (a) Cf. the summary on photoelectron spectra and bonding in phosphorus compounds by: Bock, H. *Pure Appl. Chem.* 1975, 44, 343 and literature quoted. (b) Cf. also, other calculations as reviewed by: Wedig, U.; Stoll, H.; Preuss, H. *Chem. Phys.* 1981, 61, 117.

(8) Brundle, C. R.; Kuebler, N. A.; Robin, M. B.; Basch, H. *Inorg. Chem.* 1972, 11, 20.

(9) Evans, S.; Joachim, P. J.; Orchard, A. F.; Turner, D. W. *Int. J. Mass Spectrom. Ion Phys.* 1972, 9, 41. Cf. also: Guest, M. F.; Hillier, I. H.; Saunders, V. R. *J. Chem. Soc., Faraday Trans. 2* 1972, 68, 2070.

(10) Cf. the summary on vacuum ultraviolet photoelectron spectroscopy of transient species by: Dyke, J. M.; Jonathan, N.; Morris, A. In "Electron Spectroscopy"; Brundle, C. R.; Baker, A. D., Eds.; Academic Press: London, 1979; Vol. 3, p 214 and literature quoted. For the first report of P_2 see: Potts, A. W.; Glenn, K. G.; Price, W. C. *Faraday Discuss. Chem. Soc.* 1972, No. 54, 65.

(11) Bulgin, D. K.; Dyke, J. M.; Morris, A. *J. Chem. Soc., Faraday Trans. 2* 1976, 2225.

(12) Chong, D. P.; Takahata, Y. *J. Electron Spectrosc. Relat. Phenom.* 1977, 10, 137.

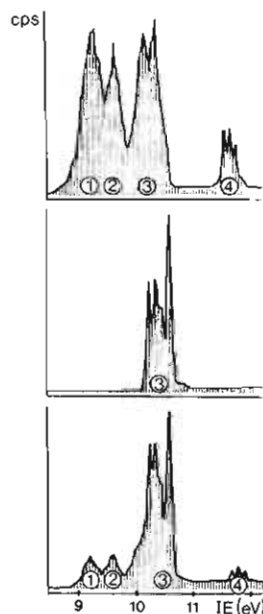


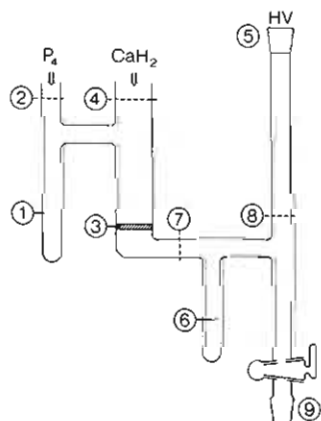
Figure 1. Computer plots of P_4 and P_2 PE spectra between 9 and 12 eV and a simulation of their 14:86 mixture (for the assignment of bands 1–4 see text).

ion-state sequence ${}^2E < {}^2T_2 < {}^2A_1 < {}^2T_2 < {}^2A_1$ for P_4^{+7-9} and ${}^2\Pi_u < {}^2\Sigma_g^+ < {}^2\Sigma_u^+ \dots$ for P_2^{+10-12} . Computer mixing of the P_4 and P_2 PE spectra—assuming comparable ionization cross sections²—suggests that the concentration of the individual components may be determined simultaneously in their gaseous mixtures (Figure 1).

Considering in addition the PE spectrometer design i.e. a flow system at reduced pressure in a helium atmosphere,² it seemed feasible to measure the temperature dependence of the equilibrium (1) by means of the advantageous PE spectroscopic real-time gas analysis² using only millimole quantities of white phosphorus, a dangerous vapor at higher temperatures, within a single day.

Experimental Section

White Phosphorus Purification and Handling.¹⁴ Commercially available white phosphorus sticks were wiped dry, rinsed with dry acetone, and transferred into tube (1) of the glass apparatus that had been browned by coating with silver mordant and consecutive tempering at 700 K:



After dry powdered CaH_2 was filled onto the glass filter plate (3) and openings (2) and (4) were sealed, the whole apparatus was evacuated to 10^{-4} mbar after connecting it to a high-vacuum (HV) line at joint (5). After trap (6) was cooled with liquid nitrogen, tube

(13) See also: Herzberg, G. "Spectra of Diatomic Molecules"; Van Nostrand: Princeton, NJ, 1950.

(14) Müller, H. Master Thesis, University of Frankfurt, 1975.

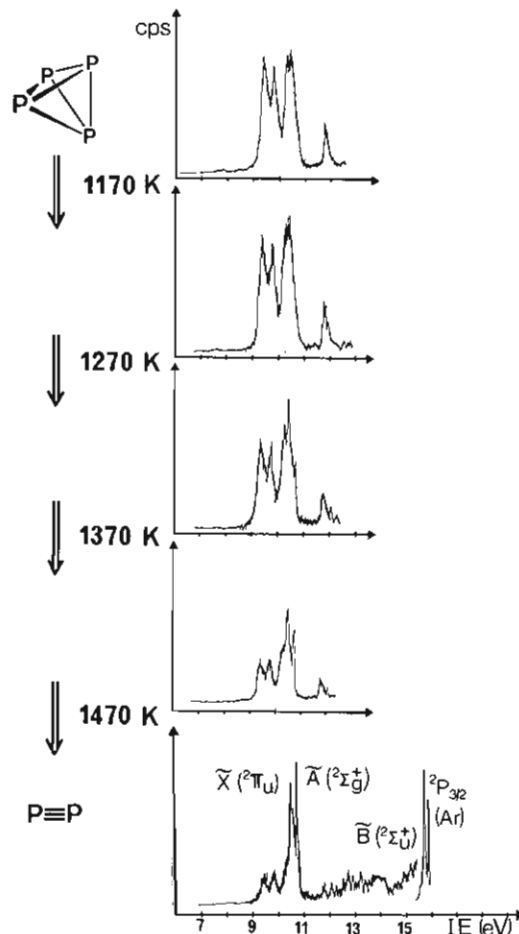
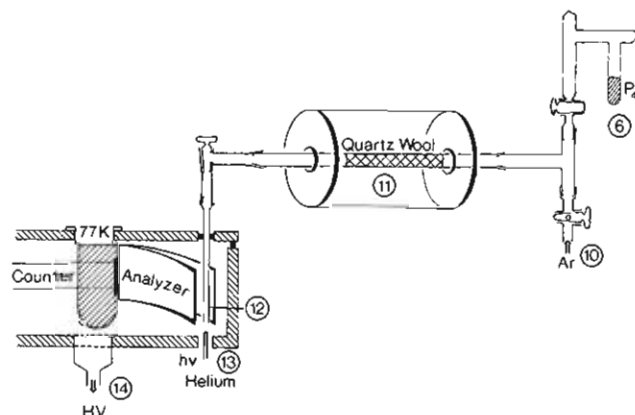


Figure 2. He I PE spectra of phosphorus vapor at 298, 1170, 1270, 1370, and 1470 K, calibrated with the ${}^2P_{3/2}$ (Ar) band at 15.76 eV (for the P_2 radical-cation state assignment; cf. Introduction).

(1) was gently heated and white phosphorus distilled through the CaH_2 layer into the storage trap (6), which was sealed off at both points (7) and (8) and connected to the PE spectrometer at joint (9).

As useful advice for the destruction of white phosphorus residues, which can be dangerous especially if they are spread out, a 1-day bathing of all used glassware in an aqueous sodium hypobromite ($NaOH + Br_2$) solution is recommended.

PE Spectroscopic Measurement. The P_4 storage trap (6) as well as an argon-carrier gas inlet (10) are both connected to the pyrolysis tube filled with quartz wool to improve heat transfer from the temperature-controlled furnace (11).



The whole set-up is evacuated on the high-vacuum (HV) diffusion pump (14) of a Perkin-Elmer photoelectron spectrometer Model PS 16, and its 77 K liquid-nitrogen cooling trap. The P_4/P_2 molecule beam from the heating zone and the photons from an open helium discharge meet in the target chamber of the PE spectrometer right in front of the slit (12) through which the emitted electrons pass via

Table I

T, K	$I_1:I_2:I_3:I_4$	$I_3(P_4)$	$I_3(P_2)$	$I_3(P_4)/I_3$	$I_3(P_2)/I_3$	% P_4	% P_2
300-1070	5:4:6:1	6	0	1	0	100	0
1120	5:3:6:1	6	0	1	0	100	0
1170	3:2:4:1	3.6	0.4	0.9	0.2	82	18
1270	4:2.5:7:1	4.8	2.2	0.69	0.63	52	48
1370	2.7:1.7:7:1	3.24	3.76	0.46	1.07	30	70
1470	4:3:20:1	4.8	15.2	0.24	1.52	14	86

Table II

T, K	α	K_P	$\ln K_P$
1170	0.1	1.49×10^{-5}	-11.11
1270	0.3	1.57×10^{-4}	-8.76
1370	0.5	6.07×10^{-4}	-7.41
1470	0.8	2.02×10^{-3}	-6.20

the analyzer into the counter. Essential for reliable measurements are (i) a distance, as short as possible, between heating zone (11) and target chamber (12), (ii) a heavy thermal insulation of the tube connecting (11) and (12), and (iii) a constant velocity of the argon carrier during registration of all PE spectra.

After a PE spectrum of P_4 was recorded at 300 K, the furnace temperature was raised in steps of 100 K as measured by a thermometer inside the furnace and, consecutively, the other PE spectra were recorded (Figure 2).

Intensity Data Analysis. For the evaluation of the $P_4:P_2$ ratios, the following procedure has been developed: According to the PE spectra of P_4 and P_2 displayed in Figure 1, the ionization bands 1, 2, and 4 belong exclusively to P_4 , whereas band 3 contains components of both P_4 and P_2 . Assuming Gaussian curve shapes, the three low-energy ionization bands of P_4 are separated in 1-3, yielding a planimetrically determined area ratio $I_3:I_1 \sim 1.2$. For mixtures of P_4 and P_2 , the band area belonging to P_2 can be approximated by $I_3(P_2) = I_3(P_4 + P_2) - 1.2I_1(P_4)$. The underlying assumption that the respective ionization cross sections are of comparable magnitude has been verified by calibration measurements varying the P_4 vapor pressure. From the band intensity ratios determined by the above procedure after normalization, $I_3(P_4)/I_3$ and $2I_3(P_2)/I_3$, the relative amounts (percent) of P_4 and P_2 can be determined (Table I).

The PE spectra between 1120 and 1470 K have been recorded within only 3 h, and under the measurement conditions a constant pressure $P = 0.28$ torr has been observed. With the PE intensities being proportional to the partial pressures (cf., e.g., Figures 1 and 2 for simulated and recorded PE spectra of a 14:86 mixture), the dissociation coefficient α introduced by

$$p(P_4) = [(1 - \alpha)/(1 + \alpha)]P \quad p(P_2) = [2\alpha/(1 + \alpha)]P \quad (2)$$

allows determination of the degree of dissociation and the dissociation constant

$$K_P = p^2(P_2)/p(P_4) = [4\alpha^2/(1 - \alpha^2)]P \quad (3)$$

at various temperatures (Table II).

MNDO Hypersurface Calculations. Starting from the known structures of P_4 ($d_{PP} = 221 \pm 2$ pm; $\angle(\text{PPP}) = 60^\circ$)⁵ and of P_2 ($d_{PP} = 189$ pm)⁶ or by using the Fletcher/Powell geometry optimization subroutine, MNDO calculations¹⁵ for P_4 and P_2 as well as for connecting hypersurfaces have been performed at the Hochschul-Rechenzentrum, University of Frankfurt.

Results and Discussion

PE Spectra at Various Temperatures. The PE spectra of white phosphorus at increasing temperatures (Figure 2) unequivocally demonstrate that P_4 is in equilibrium with increasing amounts of P_2 and that there is no indication for the formation of any other species, e.g. P atoms with $IE_1 = 10.48$ eV.¹⁶

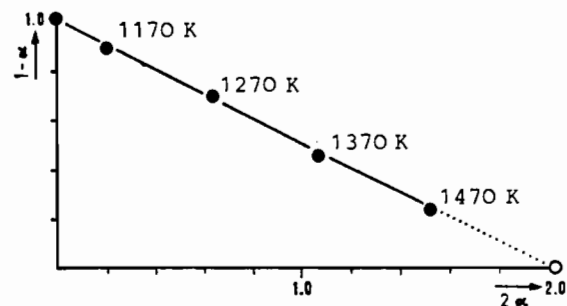


Figure 3.

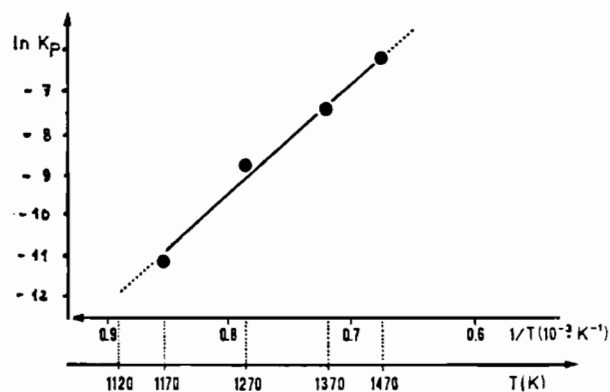


Figure 4.

From the decreasing intensities of the first two PE bands and the increasing one of the third band system (cf., Experimental Section), the degree of dissociation α and the dissociation constant K_P can be extracted (cf., Experimental Section). To begin with, a plot of the residual $(1 - \alpha) P_4$ molecules vs. the $(2\alpha) P_2$ fragments formed within the equilibrium (1) results in a straight regression line and, thus, also proves that no other species are formed under the measurement conditions (Figure 3). If finally, $\ln K_P$ is plotted vs. the reciprocal temperature (Figure 4), one obtains the regression

$$\ln K_P = -27870(1/T) + 12.895 \quad (4)$$

exhibiting the satisfying correlation coefficient $R = 0.9947$ and a standard deviation $SE = 0.27$. Although other measurements of the $P_4 \rightleftharpoons 2P_2$ equilibrium have applied other techniques and other conditions, there seems to be reasonable agreement: thus, at $P = 0.19$ and $T = 1370$ K the values $\alpha = 0.41$ and $\ln K_P' = \ln K_P/4 = -0.81$ have been reported.⁵

The temperature dependence of $\ln K_P$ (Figure 4) inserted into the thermodynamic relation $\ln K_P = -\Delta H/RT + \Delta S/R$ yields approximate values for the dissociation enthalpy, $\Delta H \sim 232$ kJ/mol, and the associated entropy difference $\Delta S \sim 107$ J/mol K, of which ΔH corresponds to the literature value of the P_4 dissociation energy, $D_0 = 217$ kJ/mol.⁶

MNDO Hypersurface Calculations. MNDO calculations for P_4 and P_2 based on their structural parameters allow, via Koopmans' theorem, $IE_n^v = -\epsilon_j^{\text{MNDO}}$, to reproduce satisfactorily their bond lengths and their PE spectroscopic ionization patterns (Figures 1 and 2):

$$P_4(d_{PP} = 221 \text{ ppm}): IE_n = 0.74(-\epsilon_j^{\text{MNDO}}) + 3.83$$

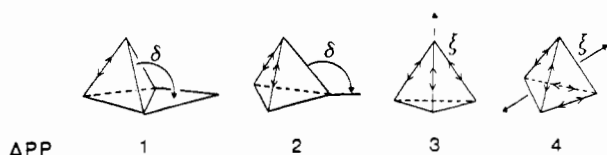
$$P_2(d_{PP} = 189 \text{ ppm}): IE_n = 1.0(-\epsilon_j^{\text{MNDO}}) - 0.08 \quad (5)$$

The linear regressions (5) exhibit the rather small standard deviations, $SE = 0.13$ and 0.10 eV, respectively, for Koopmans' correlations with semiempirical eigenvalues. The resulting eigenvalue sequences are consistent with the P_4 and P_2 radical-cation-state assignment according to ab initio SCF cal-

(15) Dewar, M. J. S.; Thiel, W. *J. Am. Chem. Soc.* 1977, 99, 5899.

(16) Cf. e.g.: "Handbook of Chemistry and Physics"; The Chemical Rubber Co.: Cleveland, OH, 1970; p E-74.

Chart I



culations.^{8,17} Therefore, we attempted to speculate about the P_4 cluster opening, which could occur in several ways by opening one to four PP edges (Chart I).

So far, only the dissociation by simultaneously breaking $\Delta(\text{PP}) = 4$ bonds has been considered in the literature.^{17,18} The analogous dimerization of nitrogen ($2\text{N}_2 \rightleftharpoons \text{N}_4$)—the difference in radical-cation ground states for N_2 , $\text{X}(^2\Sigma_g^+)$, and P_2 , $\text{X}(^2\Pi_u)$, can be neglected in qualitative orbital diagrams—has been rationalized by Pearson¹⁸ within the framework of the Woodward–Hoffmann rules.^{19,20} He demonstrated convincingly that the reaction is forbidden in D_{2d} as well as skew- D_2 symmetry due to a $b_1 \times b_2$ crossing, a point missed in ab initio calculations on the P_4 cluster opening.¹⁷

On the basis of the experimentally supported (eq 5) applicability of MNDO,¹⁵ we have screened all possibilities (Chart I) in tentative calculations by varying the respective angles δ or the reaction coordinate ζ as follows:

$\Delta\text{PP} = 1$: The length of the opening bond is increased in steps of $\Delta d_{\text{PP}} = 20$ pm up to 381 pm, while all others are kept fixed.

$\Delta\text{PP} = 2$: The angle δ is reduced to 0° by 15° increments, thereby increasing the distance along the opening bonds up to 420 ppm.

$\Delta\text{PP} = 3$: Steps of $\Delta\zeta = 30$ ppm between 180 and 380 ppm from the basal triangle have been considered, elongating the involved bonds up to 400 pm.

$\Delta\text{PP} = 4$: Among the possibilities, twisting of the dihedral angle by increments $\Delta\omega = 11^\circ$ in the direction toward a planar P_4 skeleton as well as increasing the distance between the two P_2 subunits along the C_2 axis by steps $\Delta\zeta = 30$ pm has been tested.

Of all the possibilities (Chart I) considered, the dissociation by breaking $\Delta\text{PP} = 4$ bonds simultaneously yielded the smallest increase in MNDO total energy. Obviously, this movement within the $3n - 6 = 6$ -dimensional hypersurface must occur along and between some deeper troughs and has to cross only one of the relatively lower saddles in total energy. Therefore, an additional variation of P_4 tetrahedral bond lengths has been carried out, and all the results were combined to plot the approximate hypersurface presented in Figure 5.

The barrier—calculated without configuration interaction—for the crossover between the two troughs holding the stable molecules P_4 and P_2 amounts to $E_{\text{total}}^{\text{MNDO}} \sim 177$

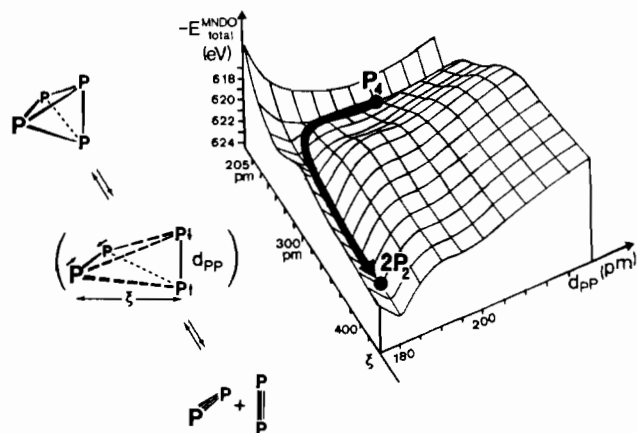


Figure 5. Section of a MNDO hypersurface generated by increasing the dissociation coordinate ζ (Chart I) and simultaneously varying all PP bond lengths (see text).

kJ/mol . Although some 40 kJ/mol below the experimental value $D_0 = 217 \text{ kJ/mol}$, the MNDO result—either by chance or due to the reliable parametrization (eq 5)—is one of the numerically closest reported so far for the $P_4 \rightleftharpoons 2P_2$ equilibrium.^{7b} As a rationale, the simultaneous opening of four bonds and shortening of two bonds—even exaggerated by the MNDO procedure down to a shallow minimum at about 169 pm—can be offered. Contrary to¹⁷ and as required by the symmetry forbiddenness quoted,¹⁸ the orbital crossing $b_1 \times b_2$ is observed. Altogether, the individual pathways (Chart I) as explored by semiempirical MNDO calculations can be discussed within the orbital correspondence analysis in maximum symmetry approach²⁰ in the following way:²¹ In D_{2d} symmetry, the four pathways (Chart I) can be labeled e for $\Delta\text{PP} = 1$ and 2, e or b_2 depending on the axis chosen for $\Delta\text{PP} = 3$, or a_1 for $\Delta\text{PP} = 4$. The forbidding crossing $b_1 \times b_2$ can be avoided, in principle, by an $a_2 (=b_1 \cdot b_2)$ displacement, i.e. within the D_{2d} subgroup S_4 . Unfortunately, however, among the six vibrational modes of P_4 in D_{2d} symmetry, which transform as $2a_1 + b_1 + b_2 + e$, there is no internal coordinate of the irreducible representation a_2 except for the rotation R_z . In second order, the only potentially useful displacement ($b_1 + b_2$) that retains some symmetry at all would reduce D_{2d} to C_2^v and should be considered more explicitly in future elaborations on the $P_4 \rightleftharpoons 2P_2$ equilibrium.

In summary, the MNDO hypersurface (Figure 5) displaying deep troughs for P_4 and P_2 provides another supporting argument for why on heating of white phosphorus up to 1470 K no other phosphorus species such as P atoms or thermodynamically presumably more favorable molecules such as P_6 or P_8 ^{21,22} could be detected PE spectroscopically (Figure 2).

Acknowledgment. The research project has been supported by the state of Hesse and the Hoechst AG. We also gratefully acknowledge the valuable discussion remarks by E. A. Halevi (Technion Haifa) as well as computational assistance by Dr. A. Semkow (University of Frankfurt).

Registry No. P_4 , 12185-10-3.

- (17) Osman, R.; Coffey, P.; Van Wazer, J. R. *Inorg. Chem.* **1976**, *15*, 287.
 (18) Cf. e.g.: Pearson, R. G. "Symmetry Rules for Chemical Reactions"; Wiley-Interscience: New York, 1976; p 62 f and 117. For the C_2H_4 hypersurface see: Kollmar, H.; Carrion, F.; Dewar, M. J. S.; Bingham, R. C. *J. Am. Chem. Soc.* **1981**, *103*, 5292. Cf. also the opening of the tetrahedrane (RC_4) cluster: Bock, H.; Roth, B.; Maier, G.; *Angew. Chem.* **1980**, *92*, 213; *Angew. Chem., Int. Ed. Engl.* **1980**, *19*, 209; *Chem. Ber.* **1984**, *117*, 172.
 (19) Woodward, R. B.; Hoffmann, R. "The Conservation of Orbital Symmetry"; Verlag Chemie: Weinheim, 1970; Academic Press: New York, 1970.
 (20) Cf. the review on orbital correspondence analysis in maximum symmetry: Halevi, E. A. *Angew. Chem.* **1976**, *88*, 664; *Angew. Chem., Int. Ed. Engl.* **1976**, *15*, 593.

- (21) Halevi, E. A., personal communication. Cf. also the following report on the symmetry-forbidden dimerization $2P_4 \rightleftharpoons P_8$: Halevi, E. A.; Bock, H.; Roth, B. *Inorg. Chem.*, companion note in this issue.
 (22) Cf., however: Trinquier, G.; Malrieu, J.-P.; Daudey, J.-P. *Chem. Phys. Lett.* **1981**, *80*, 552.